ORIGINAL ARTICLE

Box-Behnken Design Approach to Develop and Optimize Mannose-Conjugated Genistein-Loaded Transferosomal Gel

Rachana R. Yeligar[1], Vijay Kumar Singh[1], Prashanth Nayak[2], Manmohan Singh Jangdey[3], Khomendra Kumar Sarwa[4]*

[1]Shri Rawatpura Sarkar College of Pharmacy, Shri Rawatpura Sarkar University, Dhaneli, Raipur, Chhattisgarh, India, [2]Department of Pharmaceutics, NGSM Institute of Pharmaceutical Sciences, NITTE (Deemed to be University), Mangaluru, Karnataka, India, [3]Sita Ram Kashyap College of Pharmacy, Rahod, Janjgir Champa, Chhattisgarh, India, [4]Department of Pharmacy, Government Girls Polytechnic, Raipur, Chhattisgarh, India

Abstract

Objective: The present study aims to develop and optimize the mannose-conjugated genistein-loaded transferosomal gel of by Box-Behnken design to maximize entrapment efficiency, and drug loading with the lowest vesicle size. **Methods:** Mannose-conjugated genistein-loaded transferosomes were prepared by the thin film hydration method and optimised the formulation using the Box-Behnken a full factorial central composite design. The formulations were characterized for particle size, zeta potential, poly dispersibility index, entrapment efficiency and drug content. Contour plots and surface plots were used to predict the final composition of the optimized formulation of the genistein-loaded transferosome. In this optimized formulation mannose was conjugated and prepared mannose-conjugated genistein-loaded transferosomes. This vesicle system was incorporated into Carbopol 940 gel for topical delivery. The final gel formulation was characterized for homogeneity, pH, spreadability, dynamic viscosity and drug content. **Results:** The formulation has shown a particle size of 182.0 nm, PDI0.268, zeta potential -28.4 entrapment efficiency of 78.25%±0.06, and drug loading of 68.26% ± 1.23. Spherical shape particles found in the Transmission Electron Microscopic image have the mean particle size scale and were found to be in the nano-formulation range (less than 200 nm). Mannose-conjugated genistein-loaded transferosomal gel was found suitable for topical delivery with favourable pH, viscosity, spreadability and drug content. **Conclusion:** The study revealed that both genistein-loaded transferosomes and mannose-conjugated genistein-loaded transferosomes formulations were successfully optimized by Box-Behnken Design. Both the gel preparations confirming the physical characteristics parameters were found in an acceptable range.

Key words: Box-Behnken Design, transferosomes, Genistein, Mannose

INTRODUCTION

Genistein (4, 5, 7-trihydroxyisoflavone), the most biologically active and the most abundant isoflavone in soybeans, is attracting a large amount of interest because its activity is involved in a variety of health-protective effects including reducing the risk of cardiovascular disease, lowering rates of prostate cancer, inhibition of the cancerous cell growth, and improving bone health, among many other claims.[1-5]

A large number of products containing genistein are also being marketed and are available as nutritional supplements. According to the literature,[6] genistein falls in the BCS Class II of compounds, which includes compounds having low solubility and high permeability. Therefore, the limited aqueous solubility (3.04 ng/mL)[6-8] of genistein is the main hurdle for its *in vitro* dissolution profile and thus the oral bioavailability.

A ground-breaking discovery has emerged in the field of vesicle research, known as "Transferosomes" which represents a significant advancement.[9-11] This innovative delivery system exhibits remarkable properties, enabling

Address for correspondence:
Dr. Khomendra Kumar Sarwa, Department of Pharmacy, Government Girls Polytechnic, Raipur, Chhattisgarh, India. Phone: +91-78030639909.
E-mail: khomendra.sarwa@gmail.com

Received: 15-05-2024
Revised: 23-06-2024
Accepted: 29-06-2024

it to penetrate the skin more deeply and even reach the bloodstream without compromising the integrity of the vesicles.[12] Extensive investigations have confirmed that transferosomes possess the unique ability to transport active substances through the skin's protective barrier, known as the stratum corneum, leading to enhanced drug permeation.

Transferosomes, a novel vesicular delivery system, consist of amphipathic ingredients like phosphatidylcholine, which assemble themselves into a lipid bilayer when in an aqueous solution. They also include a component called the edge activator (EA), which is a bilayer softening agent, typically a biocompatible surfactant. The EA greatly enhances the flexibility and permeability of the lipid bilayer.[13,14]

The remarkable feature of transferosomes lies in their self-optimizing and ultra-deformable nature, enabling them to easily deform and pass through narrow skin constrictions that are considerably smaller than their size. This exceptional structure and composition allow transferosomes to efficiently encapsulate hydrophilic, lipophilic, and amphiphilic drugs, facilitating high drug permeation rates. In addition, they offer the potential for controlled and targeted drug delivery.[15-18]

However, a common limitation of many vesicular drug delivery systems, including liposomes, niosomes, and transferosomes, is their low viscosity, which prevents them from remaining at the application site for an extended period and makes their topical application inconvenient.[19,20] To address this issue, transferosome-based gels, referred to as transferosomal gels, have been developed. These gels enhance adhesion to the skin and enable the controlled release of transferosomes, allowing for targeted and controlled release of the bioactive agents encapsulated within the vesicles. This controlled release is often necessary to achieve the desired therapeutic effect.[21,22]

Another crucial factor to consider during the formulation development of dermal applications is the pH of the gel. Human skin typically has a pH range of 4.5–5.5.[23] The previous studies on transferosomal gel formulations have reported that the prepared formulations maintain skin-compatible pH values ranging from 5.3 to 7.6.[24-27] In the present study, a gel formulation for dermal administration of transferosomes loaded with genistein and mannose-conjugated genistein has been developed to overcome the aforementioned limitation of transferosomes and provide a therapeutic gel for treating skin cancer.

The application of a statistical experimental design to pharmaceutical formulation development has been demonstrated to be efficient and satisfactory in acquiring the necessary information to understand the relationship between independent and dependent variables in a formulation. Response surface methodology (RSM) is often used when only a few significant factors are involved in optimization. Box–Behnken design, one of the RSM designs, was applied herein because it requires fewer runs (15 runs) in a three-factor experimental design[28] among all the RSM designs and is particularly useful when extreme treatment combinations should be avoided.

In the present study, a gel formulation for dermal administration of transferosomes loaded with genistein and mannose-conjugated genistein has been developed to overcome the aforementioned limitation of transferosomes and provide a therapeutic gel for treating skin cancer.

MATERIALS AND METHODS

Materials

Genistein and mannose were purchased from Yarrow Chemicals (Mumbai, India), and Phospholipon® 90H (Soya Lecithin 90%), Tween 80, Span 80, and Propylene Glycol were purchased from Sisco Research Laboratories Pvt. Ltd (Chennai, India). All the chemicals used in the entire experiment were of analytical grade.

Formulation and development

Preliminary experiments for the determination of design space optimum vesicle size, entrapment efficiency (EE), and drug loading with high R2 are crucial for a transpersonal formulation for better delivery of the drug. Hence, they were selected as responses. The literature review suggested that the independent factors that could influence these responses were concentrations of soya lecithin, drug, and EA.[20] The preliminary experiments were carried out by preparing trial formulations to determine the design space of different factors that influenced the selected responses.

Experimental runs as per box–Behnken design

In this study, the Box–Behnken experimental design was chosen to find the relationship between the response functions and variables. Box–Behnken design is a spherical rotatable second-order design, based on a three-level incomplete factorial design. This design requires an experiment number according to $N=k^2+k+cp$, where (k) is the factor number and (cp) is the replicate number of the central point. Box–Behnken design consists of a central point and the middle points of the edges. The response equation for this model has the following form.[21]

$$y = \beta_0 + \beta_1 x_1 + \beta_2 x_2 + \beta_3 x_3 + \beta_{11} + \beta_{22} + \beta_{33} + \beta_{12} x_1 x_2 + \beta_{13} x_1 x_3 + \beta_{23} x_2 x_3$$

Where "y" is the predicted response, b0 model constant; x1, x2, and x3 independent variables; b1, b2, and b3 are linear

coefficients; b12, b13, and b23 are cross product coefficients, and b11, b22, and b33 are the quadratic coefficients.

The formulation variables contain three factors and were evaluated at three levels: The amount of (a) phospholipid: surfactant (X1), (b) sonication time (X2), and amount of RPM (X3) as independent variables. The responses chosen were vesicle size (Y1), %EE (Y2), and % drug loading (Y3). The experiments were designed using Design Expert® software (version 11.0.3.0 64-bit, Stat- Ease, Inc. Minneapolis, MN, USA)" and the layout of the design is shown in Table 1. A total of 15 formulations were designed by the software with three center points [Table 2].

Preparation of genistein-loaded transferosomes

Genistein-loaded transferosome (RH) formulations were prepared by the thin film hydration method. Initially weighed amount of soya lecithin and EA (tween 80) was taken and dissolved in a solvent mixture, that is, chloroform: methanol (1:2). Above ingredients were taken in a round bottom flask, and the dry lipid film was allowed to form by evaporating the solvent in the rotary flash evaporator (Heidolph, Schwabach, Germany) at 68°C. After the successful formation of the lipid layer, it was then placed in a vacuum oven to remove the traces of organic solvent. Then, this lipid layer was hydrated by adding the weighed amount of drug solubilized in pH 6.0 buffer (10 mL). It was then allowed to rotate for 1 h at 50°C as per Table 2, given rpm (20, 40, and 60). Then, it was allowed for swelling at room temperature for 2 h. After swelling, the formulation was sonicated using a probe sonicator for 20–40 min with a pulse of 10 min. It was then extruded through membrane filters (0.22 μ) for size reduction. After preparation, the formulation was stored in a cool, dry place.[29]

Table 1: Factors and levels

Independent Variables	Levels		
	Low–1	Medium 0	High 1
A: Phospholipid: surfactant 0 (%w/w)	85:15	90:10	95:05
B: Sonication time (min)	20	30	40
C: Rotation speed (rpm)	20	40	60
Dependent variables	Goal		
Vesicle size (Y_1, nm)	Minimum		
Entrapment efficiency (Y_2)	Maximum		
Drug loading (Y_3, %)	Maximum		

Preparation of mannose-conjugated genistein entrapped transferosomes (RHM)

The transferosomes were prepared by a thin film hydration method as previously described. Briefly, the total amount of 4% w/w of soybean lecithin and three different EAs including Tween 80 and Span 80 at the ratio of 50:50, respectively, was dissolved uniformly in ethanol to make lecithin-EA mixtures. Subsequently, 0.5% w/w of genistein and 1% mannose were dissolved in ethanol and gradually added to the lecithin-EA mixtures. Then, ultrapure water was added to top up the mixture to 100 g.[20,30]

Preparation of RH and RHM gel

The RH and RHM-loaded transferosomal gel of 1% w/w drug concentration was prepared using carbopol 940 (1% w/w) as a

Table 2: Composition of RH as given by Box–Behnken design

Std	Drug Mg	A: Phospholipid: Surfactant (% W/W)	Cholesterol mg	Chloroform mL	Methanol mL	Buffer mL	B: Sonication time (min)	C: Rotation speed RPM
1		−1	20	5	10	10	−1	0
2		+1	20	5	10	10	−1	0
3		−1	20	5	10	10	+1	0
4		+1	20	5	10	10	+1	0
5		−1	20	5	10	10	0	−1
6		+1	20	5	10	10	0	−1
7		−1	20	5	10	10	0	+1
8		+1	20	5	10	10	0	+1
9		0	20	5	10	10	−1	−1
10		0	20	5	10	10	+1	−1
11		0	20	5	10	10	−1	+1
12		0	20	5	10	10	+1	+1
13		0	20	5	10	10	0	0
14		0	20	5	10	10	0	0
15		0	20	5	10	10	0	0

gelling agent. Other components used in the preparation were glycerine 5% w/w, methylparaben 0.1% w/w, triethanolamine (TEA) few drops, distilled water q.s. The required amount of carbopol 940 was dispersed in 10 mL double distilled water. After complete dispersion, carbopol 940 solution was kept for 24 h at room temperature for swelling. A specified amount of glycerine and methylparaben was mixed with the gel. TEA was added to it dropwise.[31] An appropriate amount of optimized RH and RHM was then incorporated into the gel base with gentle stirring.[32]

Characterization of RH and RHM gel

Physical inspection

The developed RH and RHM formulations were inspected visually to assess the homogeneity of the formulations.[33]

Estimation of pH value

The pH measurement of RH and RHM gel was investigated using a calibrated digital pH meter at room temperature.[34] The pH measurement was done in triplicate and the average reading was taken.

Spreadability test

This test was evaluated to determine the spreadability of the RH and RHM gel and measure the diameters of spreading when applied to the affected area. The test is done using the horizontal plate method; by spreading 0.5 g of the RH and RHM gel on a circle of 2 cm diameter pre-drawn on a glass plate and then a second glass plate was placed. 500 weight was permitted to rest on the upper glass plate for 5 min, and then, the distance spread by the gel from the drawn circumference was measured.[35]

Viscosity study

The viscosity of the RH and RHM gel was determined using a digital viscometer (Brookfield Engineering Laboratories, USA). Spindle no.64 was used to evaluate the viscosity of the prepared RH/RHM gel at a rotation speed of 0.3 rpm.[36]

Drug content determination

Accurately, an amount of RH and RHM gel preparations equivalent to 1 mg of genistein and mannose was diluted to 10 ml using phosphate buffer pH 6.8. Then, the drug content was determined spectrophotometrically at 273 nm using a UV-vis spectrophotometer (UV 1800, Shimadzu, Japan) using a blank sample containing the same components (without the drug).[37,38] The percentage of drug content was calculated as follows:

% Drug content = (Actual amount of RH/RHM in the formulation/ Theoretical amount of RH in the formulation) × 100[39]

Evaluation of optimized formulation

Particle size, poly dispersibility index (PDI), and zeta potential

These parameters were determined using the Zetasizer Nanoseries from Malvern Instruments in Malvern, UK, and dynamic light scattering (DLS), the mean particle size, PDI, and zeta potential of nanoparticles were calculated. The data for size, PDI, and zeta potential were recorded after the samples were placed in a quote; folded capillary cell, and quote.[40]

Vesicle size analysis

The size of the vesicle was analyzed by DLS with a Malvern Zetasizer 3000 HSA (Malvern Instruments, Malvern, UK). DLS yields the mean diameter and the PDI, which is a measure of the width of the size distribution. The sample was diluted with ultra-purified water before the experiment. The measurements were performed in triplicate.[14]

Size distribution study

The size distribution study of vesicles was performed on a computerized Malvern Zetasizer inspection system (MAL, 500962, Malvern, UK) by DLS without prior sonication at room temperature.[41]

Zeta potential

Zeta potential reflects the change in electric charge on the vesicle surface and indicates the physical stability of colloidal systems, which was measured by determining the electrophoretic mobility using the Malvern Zetasizer 3000 HSA (Malvern Instruments, UK). The transferosomes were diluted with ultra-purified water before the experiment.[33]

Entrapment efficiency

The amount of free drug in the supernatant was quantified spectrophotometrically at 483 nm after centrifuging the known quantity of nanoparticulate dispersion at 10,000 RPM for 15 min using a REMI centrifuge to determine EE. The equation was used to calculate the EE.[41]

EE = (Amount of entrapped drug)/(Amount of total drug) × 100[41]

Transmission electron microscopy (TEM)

TEM analysis was used to examine the surface morphology of manufactured transferosomes (Joel, JEM-1010, Tokyo, Japan). Before being mounted into the microscope, a silicon wafer was coated with gold and air-dried at room temperature with a diluted suspension of transferosomes (transferosomes: water, 1:5) in Milli-Q water. The image was taken at a 5 kV accelerating voltage.[39]

RESULTS AND DISCUSSION

Experimental runs as per Box–Behnken design

Formulation and characterization of genistein-loaded transferosomes (RH)

The transferosomes containing genistein (RH) were prepared by thin film hydration method. The Box–Behnken design was employed for the optimization of the formulation and the result is shown in Tables 3 and 4.

Vesicle size of transferosomes

The independent variables, that is, the ratio of A: SPC: Tween 80 [Figures 1-3]. Sonication Time (X2) and rotation speed showed significant effects on vesicle size as depicted in the 3D graph [Figures 2 and 3]. As results in the perturbation curve [Figure 2b] and 3D graph [Figure 3] showed that as the ratio of SPC: Tween 80, increases, vesicle size decreased to some extent later it increased. As the sonication time increased initially, there was a decrease in vesicle size until

Table 3: Composition and response of transferosomes as per Box–Behnken design

Std	A: Phospholipid: surfactant (% W/W)	B: Sonication time (mins)	C: Rotation speed (rpm)	Vesicle size (nm)	EE (%)	%Drug loading
1	−1	-1	0	286.4	58.6	5.2
2	1	-1	0	317.3	63.6	8.4
3	−1	1	0	244.2	75.4	7.9
4	1	1	0	281.6	84.8	6.3
5	−1	0	-1	182.6	70.5	9.1
6	1	0	-1	232.6	67.5	10.5
7	−1	0	1	204.9	64.8	7.1
8	1	0	1	216.4	84.4	7.2
9	0	-1	-1	256.8	53.6	6.8
10	0	1	-1	178.3	79.6	9.8
11	0	-1	1	264.7	60.4	5.8
12	0	1	1	172.4	73.2	5.8
13	0	0	0	222.4	79.3	10.8
14	0	0	0	210.4	75.3	10.4
15	0	0	0	215.7	73.2	10.9

EE: Entrapment efficiency

Table 4: Summary of regression analysis and ANOVA

Factor	Vesicle size (adjusted R^2=0.8712)		% EE (adjusted R^2=0.9218)		%Drug loading (Adjusted R^2=0.8913)	
	β coefficient	*P*-value	*β* coefficient	*P*-value	*β* coefficient	*P*-value
Model	+216.17	0.0075	+216.17	0.0023	+10.70	0.0005
A-Phospholipid: surfactant	+16.23	0.0296	+16.23	0.0087	+0.3875	0.0469
B-Sonication time	−31.09	0.0022	−31.09	0.0001	+0.4500	0.0285
C-RPM	+1.01	0.8582	+1.01	0.1791	−1.29	0.0003
AB	+1.62	0.8394	+1.62	0.4403	−1.20	0.0022
AC	−9.63	0.2618	−9.63	0.0077	−0.3250	0.1804
BC	−3.45	0.6694	−3.45	0.0536	−0.7500	0.0157
A^2	+28.64	0.0153	+28.64	0.9353	−1.16	0.0031
B^2	+37.57	0.0051	+37.57	0.0124	−2.59	< 0.0001
C^2	−35.68	0.0064	−35.68	0.0323	−1.06	0.0045
Lack of fit	-	0.0921	-	0.7053		0.2308

ANOVA: Analysis of variance, EE: Entrapment efficiency

Table 5: Point prediction of optimized formulation

Independent factors			Responses		
A: Phospholipid: Surfactant (% W/W)	**B: Sonication Time (mins)**	**C: Rotation Speed (rpm)**	**Vesicle size (nm)**	**EE (%)**	**% rug loading**
–0.236 (88:12% W/W)	0.542 (22 min)	0.978 (20 rpm)		Predicted mean	
			174.4	76.34	10.74
				Observed mean	
			182.0	75.84	10.12
%error			4.17	1.21	–4.87

EE: Entrapment efficiency

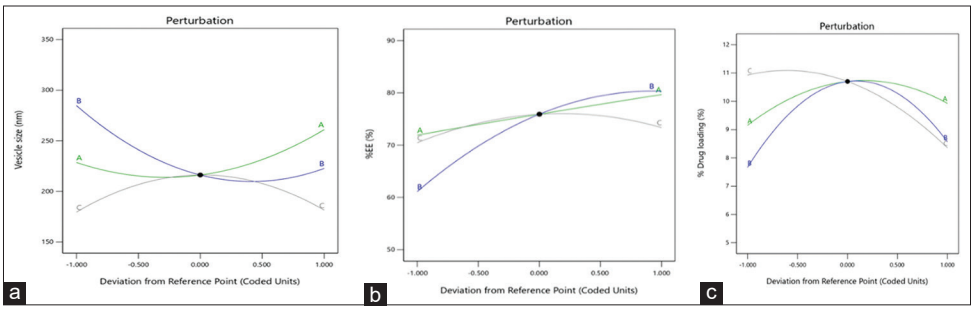

Figure 1: Perturbation curve of (a) Vesicle size (b) % entrapment efficiency and (c) % drug loading

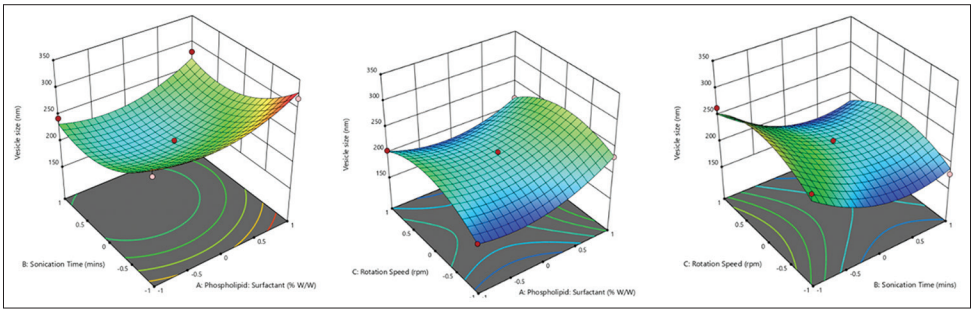

Figure 2: Response surface curve representing 3 defect of SPC: Tween 80 ratio, sonication time, and rotation speed on vesicle size

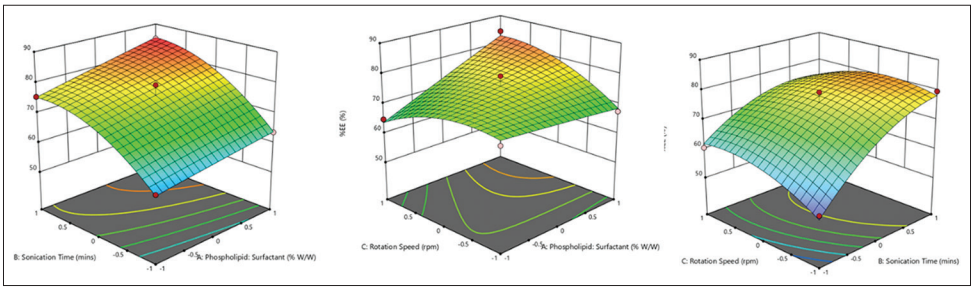

Figure 3: Response surface curve representing the 3 defect of SPC: Tween 80 ratio, sonication time, and rotation speed on % entrapment efficiency

a certain time and then the vesicle size increased at all ratios of SPC: Tween 80. Rotation speed does not affect vesicle size significantly. The size of transferosomes reduces due to the reduction in the membrane thickness and also due to the formation of a phase with interpenetrating hydrocarbon chains. The model generated for vesicle size had a $P < 0.05$ and an F value of 11.53, indicating the Quadratic model to be significant. The value of 0.092 indicates a non-significant lack of fit, implying the model to be appropriate for calculating the vesicle size. The predicted R^2 of 0.3037 is not as close to the adjusted R^2 of 0.8712 as one might normally expect; that is, the difference is more than 0.2.

The polynomial equation obtained from the results of the analysis:

Vesicle size = + 216.17 + 16.23 (A)* −31.09 (B)* + 1.01 (C) +1.62 (AB) −9.63 (AC) −3.45 (BC) +28.64 (A^2)* +37.57 (B^2)* −35.68 (C^2)*

A is the ratio of phospholipid: Surfactant, B is the sonication time, and C is the rotation speed. The coefficient in this equation reflects the standardized beta coefficient and the asterisk symbol implies variable significance. A positive sign represents an increasing effect, while a negative sign indicates a decreasing effect.

Entrapment efficiency

The 3D response surface graph [Figure 4] shows that an increase in soya lecithin concentration and decreasing surfactant concentration increases the drug's EE. With the incorporation of surfactant in low concentration, growth in vesicle size occurred, whereas a further increase in the content of surfactant may have led to pore formation in the bilayers. When surfactant concentration exceeded 15%, mixed micelles coexisted with the transferosomes, with the consequence of lower drug entrapment due to the rigidity and smaller size of mixed micelles.

The model generated for EE had a $P < 0.05$ and an F value of 19.35 indicating the Quadratic model to be significant. The value of 0.7053 indicates a non-significant lack of fit, implying the model to be appropriate to calculate the EE. The predicted R^2 of 0.7672 is in reasonable agreement with the adjusted R^2 of 0.9218; that is, the difference is <0.2. The polynomial equation obtained showed a Quadratic model from the results of the analysis:

%EE= + 75.93 + 3.87 (A)* + 9.60 (B)* + 1.45(C) + 1.10 (AB) + 5.65 (AC)* −3.30 (BC) −0.1167 (A^2) −5.22 (B^2)* −4.02 (C^2)*

A is the ratio of phospholipid: Surfactant, B is the sonication time, and C is the rotation speed. The coefficient in this equation reflects the standardized beta coefficient and the asterisk symbol implies variable significance. The polynomial equation shows that there is a positive effect of SPC: Tween 80 on the EE.

Drug loading of transferomee

% drug loading also depends on the variables of phospholipid and surfactant ratio. The present study revealed increased drug loading with phospholipid and surfactant concentrations as soon as in Figures 2 and 5. The model generated for % drug loading had a $P = 0.0005$ and an F value of 35.05, indicating that the Quadratic model was significant. The value of lack of fit is 0.2308, indicating that it is non-significant and implies the model is appropriate for calculating the % drug loading. A negative predicted R^2 implies that the overall mean may better predict your response than the current model. In some cases, a higher-order model may also predict better. The polynomial equation obtained is:

% drug loading = +10.70 + 0.3875 (A)* +0.4500(B)* −1.29(C)* −1.20(AB)* −0.3250(AC) −0.7500(BC)* −1.16(A^2)* −2.59(B^2)* −1.06(C^2)*

A is the ratio of phospholipid: Surfactant, B is the sonication time, and C is the rotation speed. The coefficient in this equation reflects the standardized beta coefficient, and the asterisk symbol implies variable significance. The polynomial equation shows a positive effect of phospholipid on the % drug loading.

Formulation and characterization of optimized batch

The optimization of transferosome was based on all the responses, with minimum particle size, PDI, and maximum EE. The optimized formula was prepared according to the solution given by the software. The predicted value of vesicle size, %EE, and % drug loading given by the software are 174.4 nm, 76.34% and 10.74%, respectively, whereas the observed value was 182.0 nm, 75.84%, and 10.12%, respectively. The observed values were within ±5% error of the predicted value, which is acceptable, as shown in Table 6 and Figure 6. The PDI of the optimized formulation was found to be 0.293, which is <0.5, meaning that the formulation is homogeneous. The predicted and observed values are summarized in Table 5.

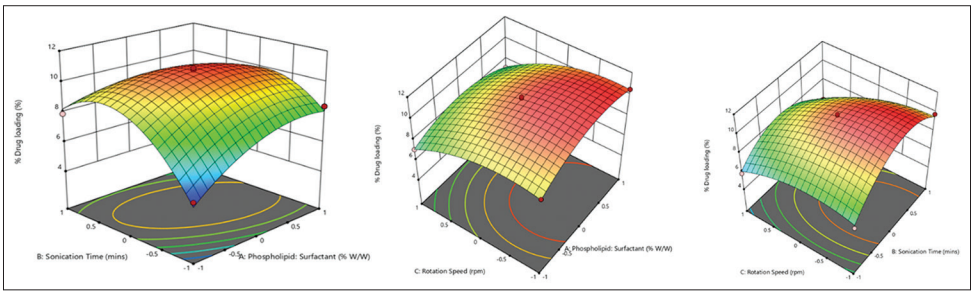

Figure 4: Response surface curve representing the 3 defect of SPC: Tween 80 ratio, sonication time, and rotation speed on % drug loading

Table 6: Formulation of physical parameters

Formulation	Homogeneity	pH	Spreadability	Dynamic viscosity (Pa.s.)	Drug content
RH	Good	6.3±0.12	+++	1118.23±2.34	68.26±1.23
RHM	Good	5.8±0.37	++++	1128.23±2.34	75.84±1.71
Transferosomes gel	Good	5.9±0.25	+++	1016±1.36	----

+++ good, ++++ very good

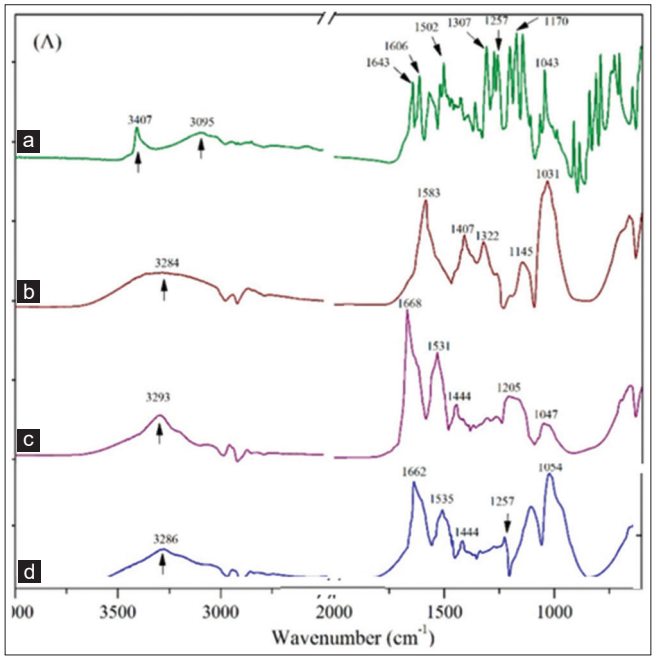

Figure 5: Fourier transform infrared spectroscopic spectra of compounds (a) physical mixture (b) genestein, (c) mannose. (d) soya lecithin

Characterization of RH and RHM gel

Physical inspection

The developed transferosomal gels exhibited a pleasant and good homogeneous appearance. There were no gritty particles and no phase separation observed in all three gel formulations. The homogeneity was detected by rubbing a small quantity of the gel on the skin of the back of the hand. The grittiness of the transferosomal gels was also observed in the same way. Both control and transferosomal gels exhibited good homogeneity, uniform consistency, and no grittiness and showed an absence of any lumps. Therefore, according to the homogeneity grading system, all three gels were graded as "good" as shown in Table 6.

The homogeneity of a topical formulation plays a crucial role in its effectiveness, as it ensures consistent drug distribution across the skin, minimizing the risk of localized over- or under-dosing. In our investigation, we found that the RH and RHM transferosome gel exhibited good homogeneity. This was evident through both visual inspection and quantitative analysis.[42]

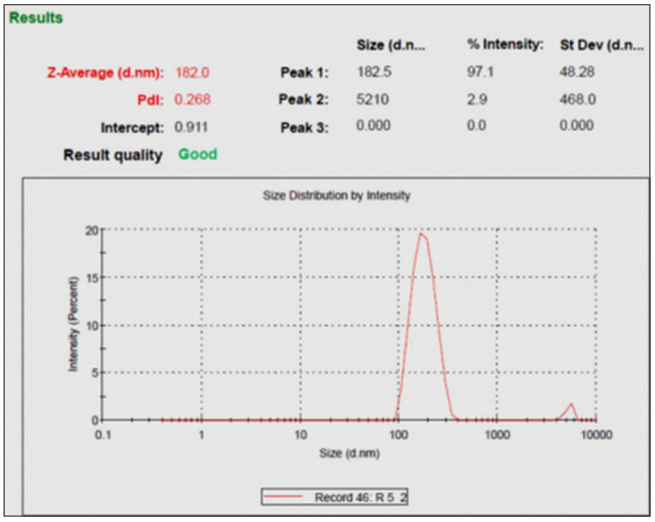

Figure 6: Size distribution of optimized formulation of genistein-loaded transferosomes

Fourier transform infrared spectroscopic studies[43]

From the above table and figure, the compounds had the functional group intact as all the group's peaks appeared in the figure; this shows that there is no physical incompatibility between the drug and the excipients, that is, genistein and soya lecithin.

Figure 5a physical mixture peaks show appear in the same range as shown in the individual spectra shown in Figure 2b. For native genistein, the apparent peaks were distributed at 3407 cm^{-1} and 3095 cm^{-1}, which could be attributed to the stretching vibrations of O-H and aromatic C–H, respectively. The C–O, C–C, C–O–C, and C–C stretching vibrations of genistein were presented at 1643, 1606, 1307–1150, and 1260–1000 cm^{-1}, respectively, (Lopez-Garcia and Ganem-Ronder, 2015). In Figure 2c, mannose peaks are seen at O-H peak at 3282 other peak at 1058 to 1658. In Figure 2d, 3278 C-H and O = H peaks seen other peaks at 1058–1656 observed of soya lecithin.

Estimation of pH value

The pH of a topical formulation is of paramount importance when considering its application to the skin. The skin's natural pH typically ranges between 4.5 and 6.0, which is slightly acidic. Deviations from this pH range can potentially disrupt the skin's barrier function and lead to irritation or discomfort. In our study, we found that the pH of the control gel (5.9) and RHM gel (5.8) was within the acceptable range

for skin compatibility, RH formulation showed an increase in pH of 6.3 which is reassuring for its use in transdermal drug delivery or cosmetic applications. The formulation's pH was carefully adjusted to match the skin's physiological pH, minimizing the risk of adverse reactions.

Spreadability test

The essence of this measurement was to ensure a uniform dose and spread of the formulation on application on the skin. In other words, the user should not experience any kind of grittiness on rubbing an applied dose of the formulation on the intact skin. This also shows that the tested polymers had good gelling properties, especially because they are all water-soluble polymers, hence the ease of formulation. In addition, they are useful excipients in industries (cosmetic, food, and pharmaceutical); hence, they are generally regarded as safe without any reactive or toxic effects spreadability of RH and transferosomal gel is found to be good as formulation RHM was found to be very good.[31]

Viscosity study

The dynamic viscosity of transferosomal gels containing genistein in both the RH and RHM formulations was a critical parameter analyzed in this study. Viscosity is a key rheological property that determines the flow behavior and spreadability of topical formulations. Understanding the viscosity of these formulations provides insights into their suitability for application, ease of spreading, and potential for sustained drug release. The dynamic viscosity measurements revealed that the transferosomal gel RH and RHM formulations exhibited distinct viscosity profiles. While the RH (1118.23 ± 2.34 Pa.s.) and transferosomal gel (1016 ± 1.36 Pa.s) formulation displayed a lower viscosity, indicating a slight fluid-like consistency, the RHM (1128.23 ± 2.34 P.as.) formulation demonstrated higher viscosity, suggesting a thicker and more gel-like texture.[44]

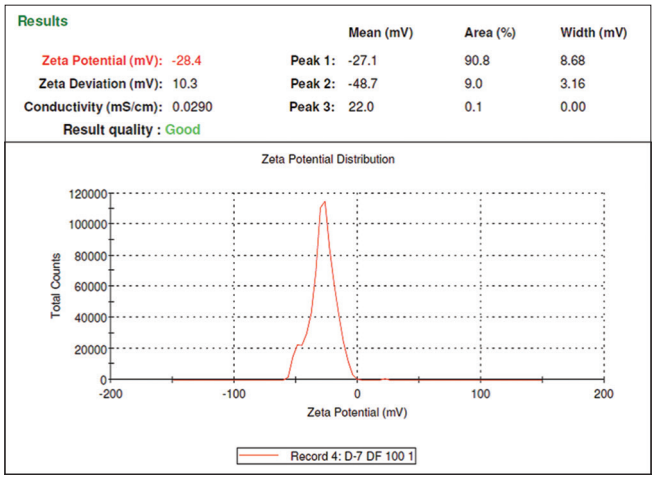

Figure 7: Zeta potential of optimized formulation of genistein-loaded transferosomes

Drug content determination

The drug content analysis for the RH transferosomal gel revealed a drug content of 68%.In contrast, the drug content in the RHM transferosomal gel was determined to be 75%. This suggests that the RHM transferosomal gel formulation contains a higher concentration of the drug compared to the RH formulation. The increased drug content in the RHM gel could have potential implications for its therapeutic efficacy and bioavailability, as a higher drug concentration may lead to a more significant local effect when applied.[45]

Evaluation of optimized transferosomes designed by RSM method

Vesicle size analysis

The RH formulation as shown in Figure 7 shows an average particle size of 182 nm and PDI of 0.268. The value implies the high-level stability of the optimized formulation. Due to the use of Tween 80, these values indicate that the particles have a neutral charge (a non-ionic surfactant). Tween 80, a surface stearic stabilizer, is used to cover the surface of nanoparticles to stop them from aggregating. The formulation would be stable as a result.

Size distribution study

As shown in Figure 7, the size distribution was in the range of 182–521 nm. The majority of nanoparticles were of the size of 182 nm; the results were nearly the same as seen in the results of DOE experiment prediction.

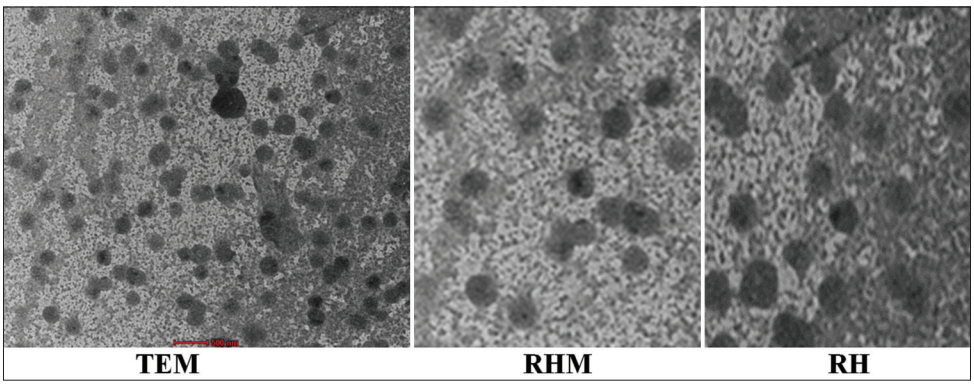

Figure 8: Transmission electron microscopic image of optimized, Left: Blank transferosomal gel, Centre: Genistein loaded transferosomal gel,Right: Mannose-conjugated genistein-loaded transferosomal gel

Zeta potential

The zeta potential of the optimized formulation RH was found to be −28.4 mV, as shown in Figure 7. The zeta potential of the transferosome showed a negative value due to the presence of surfactant. The charge of the transferosome is an important parameter that can influence both vesicular properties such as stability as well as skin-vesicle interactions.

Entrapment efficiency

Drug EE determination of the amount of drug present was found to be good in RHM formulation as compared to RH formulation which is 68.26 ± 1.23 of RH and RHM is 75.84 ± 1.71.

Transmission electron microscopy

The TEM image given in Figure 8 showed the surface morphology of vesicles with the presence of a unilamellar vesicular structure. The formed vesicles were spherical and had a vesicle size of <200 nm.[46]

CONCLUSION

The experimental results and discussions presented in this study provide valuable insights into the formulation and characterization of genistein-loaded transferosomes (RH and RHM). The Box–Behnken design was effectively employed for optimization, and the following key findings were observed, vesicle size optimization: The statistical model generated for vesicle size proved to be significant, making it suitable for predicting vesicle size based on the chosen parameters. EE was found to be influenced by the concentration of soya lecithin and surfactant. Increased soya lecithin and decreased surfactant concentration improved the EE. Beyond a certain point, excessive surfactant concentration led to lower drug entrapment due to the formation of mixed micelles and their smaller size. % Drug loading: The percentage of drug loading depended on the phospholipid and surfactant ratio. Increased concentrations of these components resulted in higher drug loading. The statistical model for % drug loading was found to be significant, indicating its applicability in predicting drug loading based on the specified parameters. The optimized formula was prepared based on minimum particle size, polydispersity index (PDI), and maximum EE. The observed values for vesicle size, % EE, and % drug loading were within an acceptable range, demonstrating the effectiveness of the optimization process. Characterization of transferosomal Gels: The physical inspection, pH, spreadability, dynamic viscosity, and drug content analysis of the transferosome gels (RH and RHM) indicated good homogeneity, skin-compatible pH, favorable spread ability, and varying viscosity profiles. The increased drug content in the RHM gel formulation could enhance its therapeutic efficacy and bioavailability. Zeta potential analysis revealed a neutral charge for the RH formulation, which contributes to its stability. The negative zeta potential of the transferosomes was attributed to the presence of surfactant, which is crucial for stability and interactions with the skin. TEM images confirmed the presence of unilamellar vesicular structures with spherical morphology and sizes of <200 nm in the optimized RH formulation, which is ideal for transdermal delivery.

In summary, this study successfully optimized the formulation of genistein-loaded transferosomes (RH) using a Box–Behnken design approach. The optimized formulation exhibited desirable characteristics for transdermal drug delivery, including vesicle size, EE, and drug loading. The transferosomes gels also showed promising physical attributes and skin compatibility, making them potentially suitable for pharmaceutical or cosmetic applications.

REFERENCES

1. Raffoul JJ, Wang Y, Kucuk O, Forman JD, Sarkar FH, Hillman GG. Genistein inhibits radiation-induced activation of NF-kappaB in prostate cancer cells promoting apoptosis and G2/M cell cyclearrest. BMC Cancer 2006;6:107.
2. Gossner G, Choi M, Tan L, Fogoros S, Griffith KA, Kuenker M, *et al*. Genistein-induced apoptosis and autophagocytosis in ovarian cancer cells. Gynecol Oncol 2007;105:23-30.
3. Xu YY, Yang C, Li SN. Effects of genistein on angiotensin-converting enzyme in rats. Life Sci 2006;79:828-37.
4. Suh KS, Koh G, Park CY, Woo JT, Kim SW, Kim JW, *et al*. Soybean isoflavones inhibit tumor necrosis factor-induced apoptosis and the production of interleukin-6 and prostaglandin E2 in osteoblastic cells. Phytochemistry 2003;63:209-15.
5. Chodon D, Ramamurty N, Sakthisekaran D. Preliminary studies on induction of apoptosis by genistein on HepG2 cell line. Toxicol *In Vitro* 2007;21:887-91.
6. Crupi V, Ficarra R, Guardo M, Majolino D, Stancanelli R, Venuti V. UV-vis and FTIR-ATR spectroscopic techniques to study the inclusion complexes of Genistein with-β cyclodextrins. J Pharm Biomed Anal 2007;44:110-7.
7. Yeligar RR, Sarwa KK, Chandrakar M, Jangde MS. Nanotechnology-based delivery of genistein to overcome physicochemical hindrance and enhance therapeutic response in skin cancer. BioNanoSci 2023;13:1339-58.
8. Paramanick D, Singh VD, Singh VK. Neuroprotective effect of phytoconstituents via nanotechnology for treatment of Alzheimer diseases. J Control Release 2022;351:638-55.
9. Opatha SA, Titapiwatanakun V, Chutoprapat R. Transfersomes: A promising nanoencapsulation technique for transdermal drug delivery. Pharmaceutics 2020;12:855.
10. Wang W, Lu KJ, Yu CH, Huang QL, Du YZ. Nano-drug delivery systems in wound treatment and skin

regeneration. J Nanobiotechnology 2019;17:82.
11. Chaurasiya P, Ganju E, Upmanyu N, Ray SK, Jain P. Transfersomes: A novel technique for transdermal drug delivery. J Drug Deliv Ther 2019;9:279-85.
12. Ahad A, Al-Saleh AA, Al-Mohizea AM, Al-Jenoobi FI, Raish M, Yassin AE, *et al*. Pharmacodynamic study of eprosartan mesylate-loaded transfersomes Carbopol® gel under Dermaroller® on rats with methylprednisolone acetate-induced hypertension. Biomed Pharmacother 2017;89:177-84.
13. Sharma VK, Sarwa KK, Mazumder B. Fluidity enhancement: A critical factor for performance of liposomal transdermal drug delivery system. J Liposome Res 2014;24:83-9.
14. Jangdey MS, Gupta A, Saraf S, Saraf S. Development and optimization of apigenin-loaded transfersomal system for skin cancer delivery: *In vitro* evaluation. Artif Cells Nanomed Biotechnol 2017;45:1452-62.
15. Walve JR, Bakliwal SR, Rane BR, Pawar SP. Transfersomes: A surrogated carrier for transdermal drug delivery system. Int J Appl Biol Pharm Technol 2011;2:204-13.
16. Sivannarayana P, Rani AP, Saikishore V, VenuBabu C, SriRekha V. Transfersomes: Ultra deformable vesicular carrier systems in transdermal drug delivery system. Res J Pharm Dosage Forms Technol 2012;4:243-55.
17. Sachan R, Parashar T, Singh V, Singh G, Tyagi S, Patel C, *et al*. Drug carrier transfersomes: A novel tool for transdermal drug delivery system. Int J Res Dev Pharm Life Sci 2013;2:309-16.
18. Sarwa KK, Mazumder B, Rudrapal M, Verma VK. Potential of capsaicin-loaded transfersomes in arthritic rats. Drug Deliv 2015;22:638-46.
19. Chen J, Ma Y, Tao Y, Zhao X, Xiong Y, Chen Z, *et al*. Formulation and evaluation of a topical liposomal gel containing a combination of zedoary turmeric oil and tretinoin for psoriasis activity. J Liposome Res 2020;31:130-44.
20. Abdellatif AA, Tawfeek HM. Transfersomal nanoparticles for enhanced transdermal delivery of clindamycin. AAPS PharmSciTech 2016;17:1067-74.
21. Pena-Rodríguez E, Moreno MC, Blanco-Fernandez B, González J, Fernández-Campos F. Epidermal delivery of retinyl palmitate loaded transfersomes: Penetration and biodistribution studies. Pharmaceutics 2020;12:112.
22. Tyagi V, Singh VK, Sharma PK, Singh V. Essential oil-based nanostructures for inflammation and rheumatoid arthritis. J Drug Deliv Sci Technol 2020;60:101983.
23. Omar MM, Hasan OA, El Sisi AM. Preparation and optimization of lidocaine transferosomal gel containing permeation enhancers: A promising approach for enhancement of skin permeation. Int J Nanomedicine 2019;14:1551-62.
24. Thakur N, Jain P, Jain V. Formulation development and evaluation of transferosomal GEL. J Drug Deliv Ther 2018;8:168-77.
25. El-Gizawy SA, Nouh A, Saber S, Kira AY. Deferoxamine-loaded transfersomes accelerates healing of pressure ulcers in streptozotocin-induced diabetic rats. J Drug Deliv Sci Technol 2020;58:101732.
26. Zhang Z, Wang X, Chen X, Wo Y, Zhang Y, Biskup E. 5-Fluorouracil-loaded transfersome as theranostics in dermal tumor of hypertrophic scar tissue. J Nanomater 2015;2015:253712.
27. Box GE, Behnken DW. Some new three level designs for the study of quantitative variables. Technometrics 1960;2:455-75.
28. Callaghan R, Luk F, Bebawy M. Inhibition of the multidrug resistance P-glycoprotein: Time for a change of strategy? Drug Metab Dispos 2014;42:623-31.
29. Garces A, Amaral MH, Sousa Lobo JM, Silva AC. Formulations based on solid lipid nanoparticles (SLN) and nanostructured lipid carriers (NLC) for cutaneous use: A review. Eur J Pharm Sci 2018;112:159-67.
30. Jangdey MS, Kaur CD, Saraf S. Efficacy of concanavalin-a conjugated nanotransfersomal gel of apigenin for enhanced targeted delivery of UV induced skin malignant melanoma. Artif Cells Nanomed Biotechnol 2019;47:904-16.
31. Nnamani PO, Ugwu AA, Nnadi OH, Kenechukwu FC, Ofokansi KC, Attama AA, *et al*. Formulation and evaluation of transdermal nanogel for delivery of artemether. Drug Deliv Transl Res 2021;11:1655-74.
32. Huang W, Dou H, Wu H, Sun Z, Wang H, Huang L. Preparation and characterisation of nobiletin-loaded nanostructured lipid carriers. J Nanomater 2017;2017:2898342.
33. Sarwa KK, Suresh PK, Debnath M, Ahmad MZ. Tamoxifen citrate loaded ethosomes for transdermal drug delivery system: Preparation and characterization. Curr Drug Deliv 2013;10:466-76.
34. Patil-Gadhe A, Kyadarkunte A, Patole M, Pokharkar V. Montelukast-loaded nanostructured lipid carriers: Part II Pulmonary drug delivery and *in vitro-in vivo* aerosol performance. Eur J Pharm Biopharm 2014;88:169-77.
35. Muller-Goymann CC. Physicochemical characterization of colloidal drug delivery systems such as reverse micelles, vesicles, liquid crystals and nanoparticles for topical administration. Eur J Pharm Biopharm 2004;58:343-56.
36. Sarwa KK, Mazumder B, Suresh PK, Kaur CD. Topical analgesic nanolipid vesicles formulation of capsaicinoids extract of Bhut Jolokia (*Capsicum chinense* Jacq): Pharmacodynamic evaluation in rat models and acceptability studies in human volunteers. Curr Drug Deliv 2016;13:1325-38.
37. Lopez-Garcia R, Ganem-Ronder V. Solid lipid nanoparticles (SLN) and nanostructured lipid carriers (NLC): Occlusive effect and penetration enhancement ability. J Cosmet Dermatol Sci Appl 2015;5:62-72.
38. Suryawanshi VK, Sarwa KK, Narayan SS. A novel rosuvastatin calcium cow ghee fraction biform complex: Formulation characterization and evaluation. Drug Deliv Lett 2021;11:307-24.

39. Sarwa KK, Patel D, Uraon D, Jangde MS, Suryawanshi VK, Saraf S. Nanoparticulate delivery systems for phytoconstituents. In: Rudrapal M, editor. Phytoantioxidants and Nanotherapeutics. United States: Wiley; 2022. p. 121-38.
40. Verma VK, Zaman MK, Verma S, Verma SK, Sarwa KK. Role of semi-purified andrographolide from *Andrographis paniculata* extract as nano-phytovesicular carrier for enhancing oral absorption and hypoglycemic activity. Chin Herb Med 2019;12:142-55.
41. Sarwa KK, Rudrapal M, Mazumder B. Topical ethosomal capsaicin attenuates edema and nociception in arthritic rats. Drug Deliv 2015;22:1043-52.
42. Nnamani PO, Kenechukwu FC, Dibua EU, Ogbonna CC, Monemeh UL, Attama AA. Transdermal microgels of gentamicin. Eur J Pharm Biopharm 2013;84:345-54.
43. Peltonen L, Hirvonen J. Pharmaceutical nanocrystals by nanomilling: Critical process parameters, particle fracturing and stabilization methods. J Pharm Pharmacol 2010;62:1569-79.
44. Elnaggar YS, Talaat SM, Bahey-El-Din MB, Abdallah OY. Novel lecithin-integrated liquid crystalline nanogels for enhanced cutaneous targeting of terconazole: Development, *in vitro* and *in vivo* studies. Int J Nanomedicine 2016;11:5531-47.
45. Maji R, Omolo CA, Jaglal Y, Singh S, Devnarain N, Mocktar C, *et al*. A transfer some-loaded bigel for enhanced transdermal delivery and antibacterial activity of vancomycin hydrochloride. Int J Pharm 2021;607:120990.
46. Das B, Sen SO, Maji R, Nayak AK, Sen KK. Transferosomal gel for transdermal delivery of risperidone: Formulation optimization and *ex vivo* permeation. J Drug Deliv Sci Technol 2017;38:59-71.

Source of Support: Nil. **Conflicts of Interest:** None declared.